

Simone Tanelli^{1*}, Jonathan Meagher, Stephen L. Durden¹ and Eastwood Im¹
¹ Jet Propulsion Laboratory, California Institute of Technology, Pasadena CA, USA

1. INTRODUCTION

The NASA/JPL airborne precipitation radar APR-2 (cross-track scanning, dual frequency - 14 and 35 GHz, Doppler and dual polarization, see Sadowy et al. (2003) for detailed description of the instrument) was operated on the NASA P-3 aircraft during the Wakasa Bay (Japan) experiment. The experiment conducted jointly by the U.S. AMSR-E and Japanese AMSR teams in Jan/Feb 2003, was designed to (1) validate both the AMSR and AMSR-E shallow rainfall and snowfall retrieval capabilities (2) extend the database of rainfall properties needed to implement a comprehensive physical validation scheme, and (3) extend our understanding of rainfall structures through the use of new remote sensing technology. On 12 flights, more than 30 hours worth of precipitation systems were observed, including rain and snow events, both over ocean and over land.

On 8 of these flights, APR-2 observed stratiform rain and the associated melting layer, whose impact on passive remote sensing of precipitation is one of the specific issues addressed by this experiment. In this study the signatures of the melting layer on APR-2 measurements from four flights are presented and discussed.

2. OBSERVATIONS AND DISCUSSION

APR-2 operates at 13.4 GHz (Ku band) and 35.6 GHz (Ka band). Copolarized power (HH), crosspolarized power (HV) and mean Doppler velocity (v) data are collected at both frequencies.

Figure 1 shows the typical multiparametric data collected (at nadir) from a stratiform event. Panels a and b show the equivalent reflectivity expressed in dBZ as calculated from HH. Calibration of Ku band was verified examining the measured backscatter cross section at 10° incidence angle under clear conditions. The average normalized cross section σ_{HH}° over all flight days was 7.5 dB which is in good agreement with previous studies. Calibration of Ka band was verified comparing the dual-frequency backscattered power of very light rain in non-attenuated conditions (*i.e.*, where backscattering is in Rayleigh regime at both frequencies and therefore equal reflectivity is expected). In this example the typical peaked brightband signature at Ku band is evident between 1.5 and 2 km altitude (*i.e.*, maximum brightband reflectivity $Z_{eBB} > Z_{eRAIN}$, the reflectivity of rain below the brightband). On the other

hand, the brightband signature at Ka band is significantly weaker ($Z_{eBB} \sim Z_{eRAIN}$) because of the weaker sensitivity of Ka band to the large wet-ice particles that cause the peak at lower frequencies. Also, the effect of attenuation at Ka band is evident in the area of strongest precipitation. Panel c shows the vertical velocity measured from the Doppler return of the Ku band signal. The sharp increase in vertical velocity (from approximately 2 m s^{-1} to 7 m s^{-1}) is due to the increased fall speed of the liquid hydrometeors with respect to the frozen ones and it takes place immediately below the brightband. Disruption of the brightband caused by light convection is visible in the first 2 minutes of observation). Panels d and e show the Linear Depolarization Ratio at the two frequencies. The sensitivity thresholds for LDR measurements are -30 dB for Ku band and -17 dB for Ka band. Significant returns are observed only near the melting layer because of the presence of wet-ice particles. Finally, panel f shows the flight track, the green and red circles correspond to the beginning and end of the sampling period, respectively.

Table 1 shows the mean and standard deviation of 5 melting layer parameters from 10 segments of APR-2 nadir observations collected on January 19th, 21st, 23rd and 27th, 2003. In generating the statistics of Table 1, only data with a measured LDR_{Ku} peak were used (for a total of 4233 sample profiles). Statistics calculated from LDR_{Ka} and v were further limited to data where those parameters were available. The maximum altitude of the brightband was observed at almost 3 km on Jan 23rd, the minimum altitude was observed at 0.5 km (right above the sea surface signature) on Jan 21st. The negative correlation (~ -0.5) between brightband altitude (h_{BB}) and maximum brightband reflectivity (Z_{eBB}) observed in previous studies (*e.g.*, Durden et al. 1997) and attributed to the cooling effect of the melting process was confirmed within each segment but the one in Jan 21st, where the brightband rose gradually from the sea level up to around 1.5 km because of the

PARAMETER	Jan 19	Jan 21	Jan 23	Jan 27
Z_{eBB} Ku	31/7	34/8	34/7	33/10
h_{BB} Ku	1.6/0.1	1.4/0.2	2.2/0.15	2.0/0.2
LDR_{BB} Ku	-19/4	-17/4	-18/4	-18/5
Z_{eBB} Ka	24/5	27/5	27/5	26/7
LDR_{BB} Ka	-13/2	-13/2	-12/2	-13/3

Table 1 Melting layer parameters grouped by day (mean/std. dev.). Z_{eBB} are the maximum observed reflectivities (dBZ), LDR_{BB} are the maximum observed Linear Depolarization Ratios (dB) and h_{BB} is the altitude at which the Z_{eBB} at Ku band was observed (km).

* Corresponding author address: Simone Tanelli,
 Jet Propulsion Laboratory, 4800 Oak Grove Dr.
 MS 300-243, Pasadena CA 91109;
 e-mail: simone.tanelli@jpl.nasa.gov

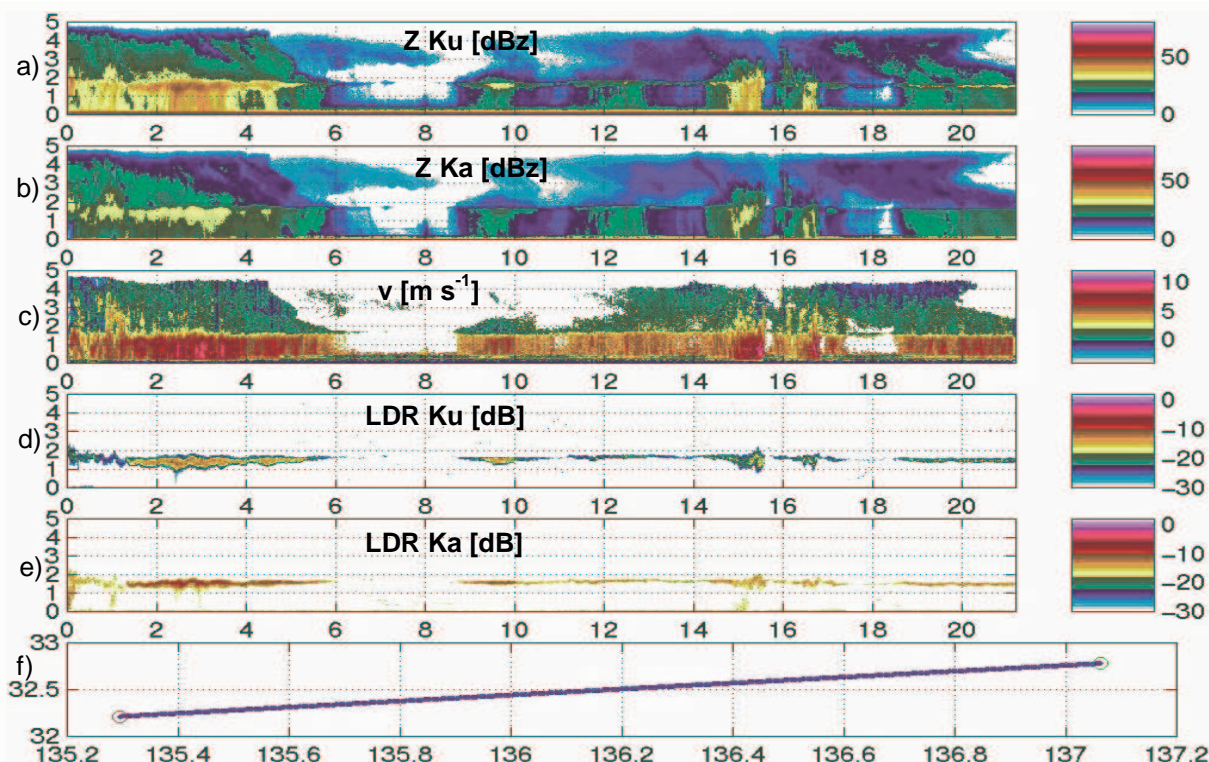


Figure 1 : Observation segment #1: starting at 05:43 UTC on Jan. 19th 2003. Panels a – e, the time of observation (in minutes from the beginning at 05:43 GMT of Jan 19th, 2003) is shown in the horizontal axis and the altitude (in km a.s.l.) is on the vertical axis. In panel f, the horizontal axis is the longitude (degrees E) and the vertical axis is the Latitude (degrees N).

changing mesoscale conditions.

Overall, the conclusions drawn in Durden et al. (1997) from TOGA COARE were confirmed by the Wakasa Bay Experiment. In particular it was observed:

- the positive correlation between Z_{eBB} Ku and brightband thickness ($\sim +0.7$);
- the negative altitude offset of the peak in LDR with respect to the peak in Z_e Ku (observed mean offset = -70 m, negatively correlated with Z_{eBB} Ku). Furthermore, a strong (~ 0.8) correlation of the altitude and thickness of the LDR signature was observed with the area of vertical acceleration of the

particles (see e.g., sample profiles in Figure 2). This seems to confirm the interpretation offered in that study for the possible cause of the negative altitude offset. On the other hand, the altitude of Ka band LDR peak was in general between that of the reflectivity peak and the Ku band LDR peak, and it showed a weaker correlation with Z_{eBB} . This might be due to the fact that smaller particles reach their terminal velocity higher than the larger particles.

- ice reflectivity above the bright band is less than rain reflectivity below; the difference becomes more negative with increasing rain reflectivity;

ACKNOWLEDGMENT

The research described in this paper was performed at the Jet Propulsion Laboratory, California Institute of Technology, for the AQUA/AMSR-E validation program under contract with the National Aeronautics and Space administration.

REFERENCES

Sadowy G.A., et al. , Development of an advanced airborne precipitation radar, *Microwave Journal*, **46**, n 1, January, 2003

Durden S.L. et al., ARMAR observations of the melting layer during TOGA COARE, *IEEE Trans. on Geosc. and Rem. Sens.*,**35**, 1997

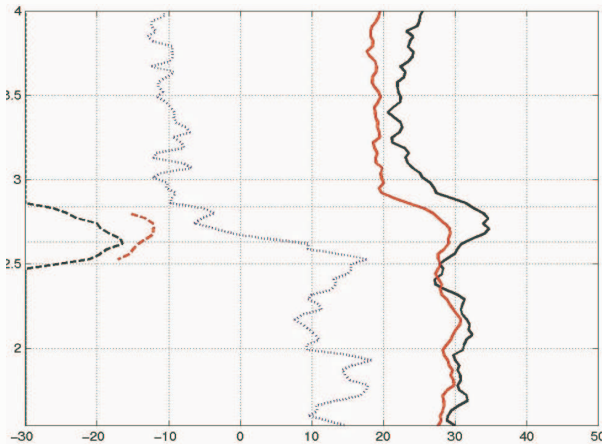


Figure 2. Vertical profiles (taken Jan 23rd) of Z (solid, in dBZ), LDR (dash, in dB) and vertical velocity (dot, in units of 0.2 m s^{-1} and shifted by -20). Colors are: black for Ku band and red for Ka band.